Available online at www.CivileJournal.org

Civil Engineering Journal

(E-ISSN: 2476-3055; ISSN: 2676-6957)

Vol. 11, No. 06, June, 2025

Effect of Axial Load on the Seismic Performance of Steel Reinforced Concrete Beam-Column Joint

Data Iranata [1*], Budi Suswanto [1], Aniendhita Rizki Amalia [1], Yuyun Tajunnisa [1], Yanisfa Septiarsilia [1, 2]

[1] *Department of Civil Engineering, Institut Teknologi Sepuluh Nopember, Surabaya 60111, Indonesia.*

[2] *Department of Civil Engineering, Institut Teknologi Adhi Tama Surabaya, Surabaya 60117, Indonesia.*

Received 04 February 2025; Revised 29 April 2025; Accepted 05 May 2025; Published 01 June 2025

Abstract

Steel-reinforced concrete (SRC) provides numerous advantages, such as enhanced energy dissipation, ductility, stiffness, and strength, particularly in seismic performance. Several studies on the effect of axial loads on columns found that axial loads have an insignificant influence on column capacity, though they influence long-term performance. Beam-column joint elements are among the critical components that determine the seismic behavior of a structure. Inaccurate design of these joints can lead to fatal structural damage, potentially causing structural collapse. This study aimed to perform a numerical analysis of various joint configurations under cyclic and axial loads to identify models with the best seismic performance that consisted of four models using different SRC length parameters. The research used nonlinear finite element methods with the ABAQUS software, which enables detailed simulations of joint behavior, including predictions of failure mechanisms that are difficult to observe in experimental testing. The results of the analysis showed that the CS-02 model demonstrated the best seismic performance. Axial load increased the capacity in all models, improved energy dissipation in the RC model, slightly reduced dissipation in CS models, and caused different rotational behavior across models.

Keywords: Beam-Column Joint; Steel Reinforced Concrete; Cyclic Load; Axial Load; Seismic Performance; Numerical Analysis.

1. Introduction

Steel-concrete composite structures have been widely applied in various countries due to their numerous advantages over conventional concrete, including improved structural strength, ease of construction, and cost efficiency. These benefits are achieved by using high-quality materials and reducing the required cross-sectional area of structural elements [1, 2]. Composite elements, such as Concrete-Encased Steel (CES), also known as Steel Reinforced Concrete (SRC), consist of Reinforced Concrete (RC) combined with either partially or fully encased steel (Figure 1). Steel-reinforced concrete is considered to enhance the structural behavior of steel, making it more effective and resistant to local buckling. The combination of steel and reinforced concrete offers several benefits, including improved energy dissipation, ductility, stiffness, and strength, particularly in seismic performance [2-5]. Steel-reinforced concrete composite structures, recognized for their exceptional mechanical performance, have become a key global research focus, with numerous studies exploring their reliability [6].

* Corresponding author: data@its.ac.id

http://dx.doi.org/10.28991/CEJ-2025-011-06-016

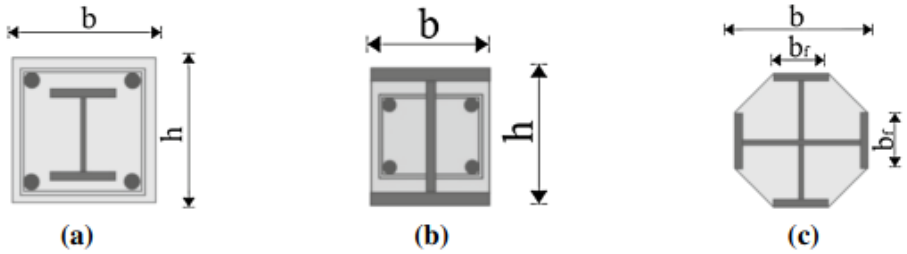

Figure 1. The cross-section of composite SRC columns: (a) Fully encased SRC column with H-shaped steel, (b) Partially encased SRC column with H-shaped steel (c) Partially encased SRC column with cross-shaped steel [2]

In the context of seismic performance, joint elements are designed as rigid connections within a special moment resisting frame (SMRF). These joints must maintain their strength and capacity under seismic forces, making SRC highly suitable for seismic-prone areas. The presence of steel reinforcement in these joints helps absorb energy, prevent abrupt failures, and enhance structural resilience [7]. Current research focuses extensively on SRC joint elements applied in high-seismic regions [3, 8]. These joint elements are critical in determining a structure's seismic behavior. Inadequate design of these joints can lead to fatal structural damage, potentially causing structural collapse [9-18]. In detail, early flexural failure in columns, shear failure in beams, or joint area failure can threaten the overall frame response, resulting in reduced structural performance. These issues have driven extensive research into developing new approaches to enhance structural performance under seismic loads [19]. Under the influence of seismic forces, beam-column joint elements must be carefully detailed to address the complex forces in the joint area, including shear reinforcement and anchorage [20]. Beam-column joints are essential for transferring forces such as shear, moments, and torsion from beams to columns [21, 22]. Therefore, beam-column joint elements must be precisely designed to ensure satisfactory performance and avoid failure before beam or column failure [23]. The structure's ductility influences its ability to withstand seismic loads, even when elements undergo plastic deformation during an earthquake. The joint's strength capacity depends on the joint type, confinement, and anchorage detailing. SRC joints with embedded steel columns can absorb shear forces effectively. The force and deformation mechanisms occurring in joint elements are illustrated in Figure 2 to represent the mechanisms. The joint area experiences complex stress distribution caused by bending moments, axial forces, and shear forces. During cyclic forces, concrete under compression may crush, and concrete under tension may crack. The beam elements also influence the failure mechanism; thus, selecting the type of joint and detailing the connections must be done carefully [19, 24]. Consequently, researchers have consistently concentrated on creating dependable joint connections with excellent seismic performance [25].

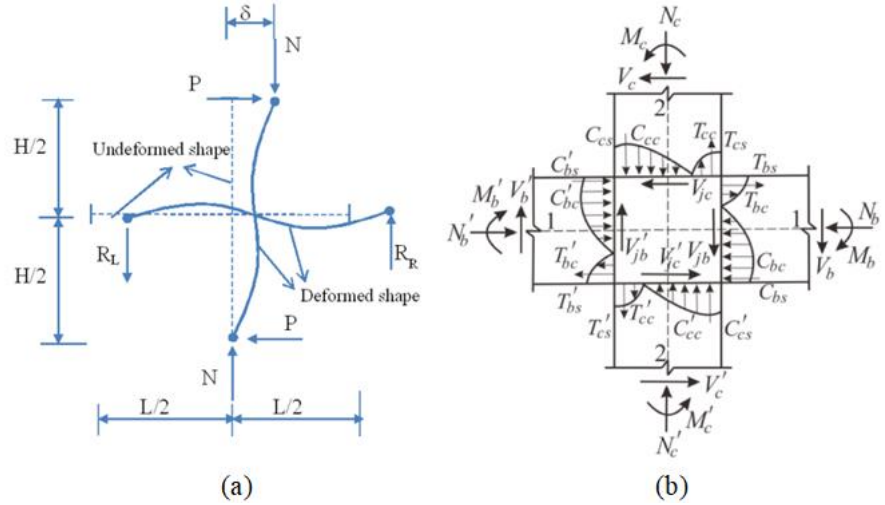

Figure 2. The force mechanism in beam-column joint elements: (a) The ideal deflection shape of a beam-column joint under cyclic and axial loading, (b) Forces acting on the beam-column joint element [19, 24]

Several studies have been conducted on SRC composite joints, exploring their effectiveness in enhancing seismic performance. Le et al. (2020) [3] investigated SRC in partially encased columns with steel beams, demonstrating that SRC can improve ductility and energy dissipation while maintaining overall structural behavior. Sermet et al. (2020) [8] compared several types of SRC in columns and partially encased beams, incorporating different axis orientations in steel beams and columns embedded in concrete. Ghayeb et al. (2022) [26] studied the development of SRC into hybrid joints, finding that SRC joints have greater deformation capacity and less damage than conventional joints. Wu et al. (2020) developed SRC columns and hybrid joints for easy assembly and installation. Choi et al. (2013) [27] researched SRC

joints as precast concrete and found that the developed joint strength was 15% higher than that of conventional joints. Based on these studies, it can be concluded that SRC joints can be further developed for stronger performance and more diverse applications, making them suitable for precast structures to facilitate faster construction. In the various studies, there is still a lack of research on SRC joints focusing on embedded steel configuration, especially regarding embedded steel length.

In addition to cyclic loads, axial loads are present in actual service conditions, including live and dead loads. Columns made of conventional reinforced concrete (RC), particularly in high-rise buildings, have limitations in resisting axial loads caused by gravitational forces. To address this issue, column dimensions must be increased, which impacts building costs and reduces usable floor space [2]. SRC columns offer an ideal solution, as they can improve strength and ductility without increasing dimensions. Several studies have been conducted on the effect of axial loads. Studies concluded that axial loads have minimal effects on column capacity but may influence long-term performance. This remains a topic of debate among researchers, prompting ongoing investigations [2, 28, 29]. Some studies showed that the axial load ratio significantly impacts joint behavior, failure mechanisms, deformation capacity, and ductility [30]. According to Gan et al. (2023) [31], axial loads enhance bonding behavior. Li et al. (2015) [32] compared beam-column joint behavior under axial load ratios of 0.2 and 0.6, finding that joints with lower axial loads exhibited greater strength capacity, drift ratio, and initial stiffness than those with higher axial loads. Similarly, Al-Osta et al. (2018) [33] conducted experimental and numerical studies on the effects of axial load ratios ranging from 0 to 0.7 of column capacity. Their findings showed that beam-column joints with high axial load capacity increased initial stiffness, but once stiffness degradation began, the rate of decline was faster. Haach et al. (2008) [34] revealed that axial loads made joint elements stiffer but reduced stresses in longitudinal reinforcement. Based on these studies, axial loads play a significant role in joint element performance and should not be underestimated. Bindhu et al. (2009) [35] found that increasing axial loads in columns enhanced load-bearing capacity and joint strength but reduced energy absorption capacity and joint ductility. In summary, the impact of axial loads on beam-column joint performance is highly complex and should not be overlooked. Further research on axial load testing is crucial to better understand beam-column joint behavior, especially under actual conditions in high-rise buildings. There remains a gap in research comparing the seismic performance of SRC beam-column joints under different axial load conditions.

This study aimed to address this research gap by conducting a numerical analysis of steel-reinforced concrete (SRC) beam-column joints with various joint configurations, including reinforced concrete (RC) joints as control models. The research highlighted the structural behavior of beam-column joints under various loading conditions. Parameters analyzed included the configuration of embedded steel within the concrete joints and cyclic loading accompanied by an axial load of $0.15f'_cA_g$. For comparison, simulations were also performed without applying axial loads to observe their significant impact on joint performance. The numerical analysis was carried out using the finite element method (FEM) implemented through the ABAQUS software, enabling accurate simulation of the nonlinear behavior of materials and structures. This approach produced numerical models representing the mechanical response of SRC and RC beam-column joints, including strength, energy dissipation, deformation, and stress distribution under cyclic loading. This study aimed to provide a more comprehensive understanding of the performance of SRC beam-column joints and serve as a valuable reference for developing more optimized joint designs for seismic-resistant building structures.

2. Novelty and Significance

This study presented a novel exploration of the impact of axial loads on the seismic performance of steel-reinforced concrete (SRC) beam-column joints through the development of three embedded steel configurations: CS-01 (steel embedded along the plastic hinge zones of column and beam elements), CS-02 (steel embedded in the beam element along the plastic hinge zones and throughout the column element), and CS-03 (steel fully embedded along the entire beam and column elements) and one control model names RC (reinforced concrete) that is a monolith joint. This approach enables a detailed analysis of the role of steel configurations in improving the load capacity, stiffness, ductility, and energy dissipation of SRC beam-column joints, an underexplored area. Furthermore, this study highlights the effect of an axial load of $0.15 f'_cA_g$, representing actual conditions in high-rise buildings. It compares it with conditions without axial loads to understand how axial loads influence joint failure mechanisms. The research was conducted using nonlinear finite element methods using the ABAQUS software, which facilitates detailed simulations of joint behavior, including predictions of failure mechanisms that are difficult to observe in experimental testing. Before modeling the development of the model, validation was conducted on previous research, specifically the study by Sermet et al. (2021) [8]. The findings of this study contributed to recommendations for optimal SRC joint designs, particularly in enhancing deformation resistance and seismic capacity for buildings in seismic-prone regions. This study also provided an important basis for further research on strengthening SRC joints and evaluating composite materials in the context of seismic-resistant structures. The research compared the results of each model in terms of strength, energy dissipation, stress distribution, and moment-rotation relationships, aiming at assisting engineers in developing appropriate, feasible, and efficient structural joint enhancement techniques for poorly designed building frames, especially in seismic-prone areas. The research stages are illustrated with a flowchart in Figure 3.

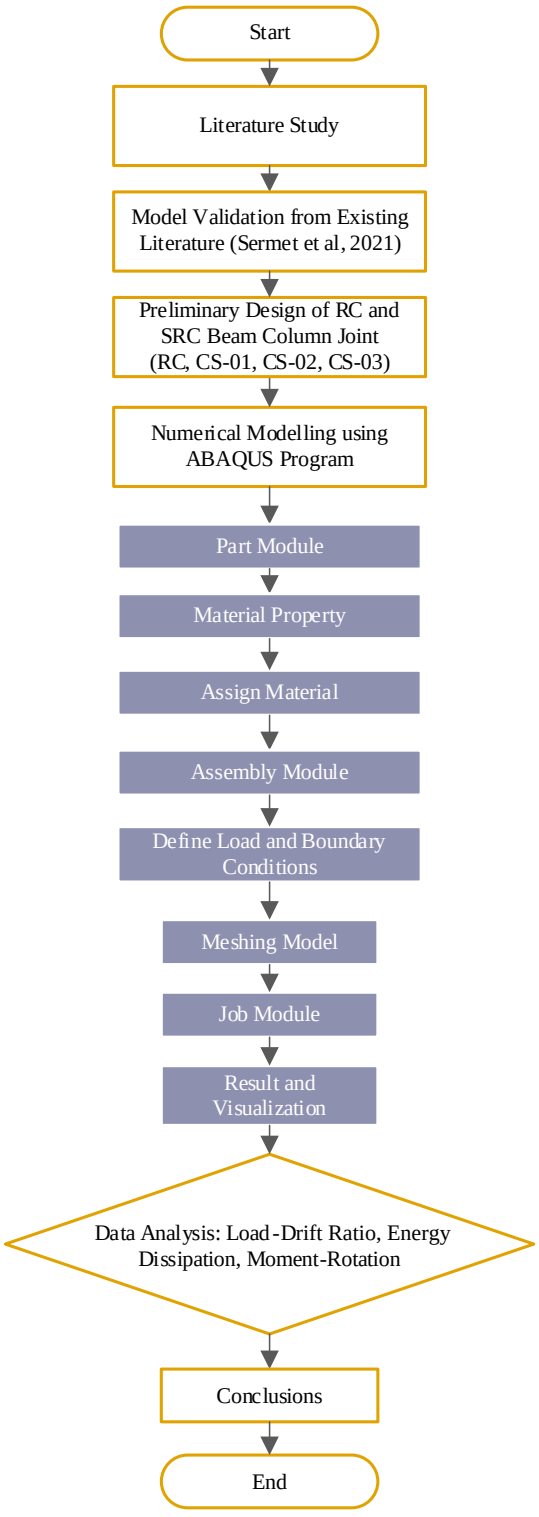

Figure 3. Flow Chart of Study Workflow

3. Material and Methods

The finite element model (FEM) is a practical and efficient analytical method for evaluating structural behavior. Using finite element simulations addresses various limitations of experimental testing, such as the high costs of full-scale testing, the extended time required to prepare complex geometries and apply loads, and the matter of accuracy [36, 37]. FEM is a numerical approach used to solve equations. Generally, material behavior can be represented using equations in differential or integral form. Therefore, FEM is recognized in mathematics as a computational technique for solving partial differential equations or integral equations [38]. Finite element analysis software was utilized to evaluate the performance variations of the innovative joint under various conditions [39]. Accurate modeling requires material data, particularly parameters for damage under plastic conditions, to enable precise computer simulations. This study employed the ABAQUS software, which can simulate the nonlinear behavior of both concrete and steel.

3.1. Material Properties of Concrete Model

Birtel & Mark (2006) [40] proposed the concrete damage plasticity (CDP) model to simulate the nonlinear behavior of concrete materials. The material functions and corresponding parameters were derived and verified using experimental data from uniaxial, biaxial, or triaxial (cyclic) stress tests. The CDP model was chosen for its capability and potential to model reinforced concrete in various structural types, effectively representing the nonlinear behavior of beam-column joints. Additionally, this model accounts for the concept of elasticity with isotropic damage and isotropic tensile and compressive plasticity, including elastic stiffness degradation caused by plastic strain under both tension and compression conditions. The CDP model is also capable of representing the characteristics of material damage. The primary failure mechanisms assumed in this model are cracking resulting from tension and crushing caused by compression. Various parameters required for the CDP model have been studied and determined based on the available literature [37, 41, 42].

The compressive damage component d_c is shown in Equation 1 with respect to the corresponding plastic strain, where the condition of inelastic strain is determined using the factor b_c with $0< b_c \leq 1$.

$$d_c = 1 - \frac{\sigma_c \, E_c^{-1}}{\varepsilon_c^{pl}\left(\frac{1}{b_c}-1\right)+\sigma_c \, E_c^{-1}} \quad (1)$$

where d_c is compressive damage, σ_c is compressive strength, ε_c^{pl} is plastic strain, E_c is modulus elasticity, and b_c is 0.7.

As with Equation 1, the damage d_t is influenced by the experimentally determined parameter $b_t = 0.1$. Consequently, it is assumed that that load returns to its initial point, resulting in minimal residual strain. The equation governing tensile failure is provided in Equation 2.

$$d_t = 1 - \frac{\sigma_c \, E_c^{-1}}{\varepsilon_t^{pl}\left(\frac{1}{b_t}-1\right)+\sigma_t \, E_c^{-1}} \quad (2)$$

where d_t is tensile damage, σ_t is tensile strength, ε_t^{pl} is plastic strain, E_c is modulus elasticity, and b_t is 0.1.

The Concrete Damage Plasticity parameters for concrete with a strength of 30 MPa from calculation are presented in Figure 4.

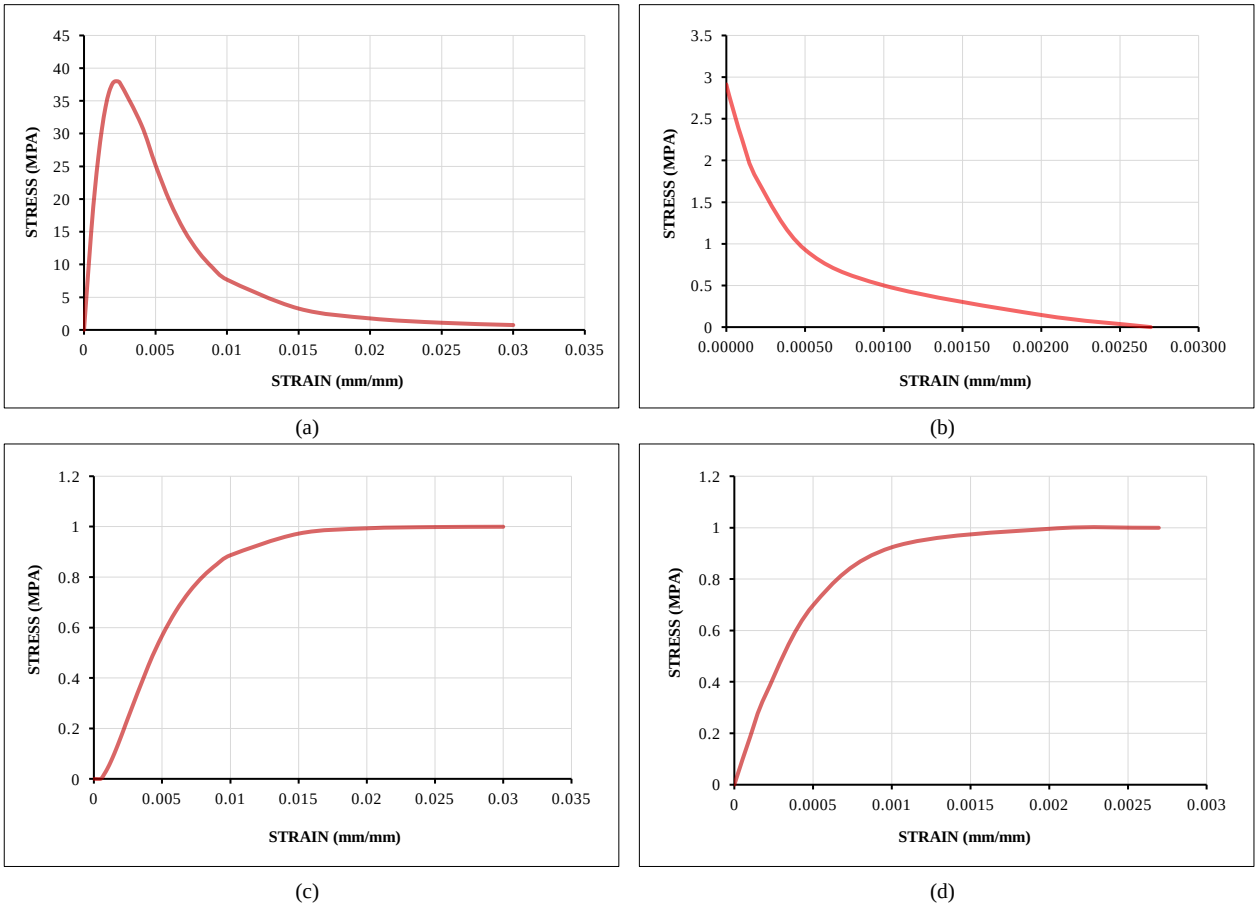

Figure 4. Concrete Damage Plasticity Parameters (Concrete Strength 30 MPa): (a) Compressive Stress vs. Strain (b) Tension Stress vs. Strain (c) Compressive Damage vs. Strain (d) Tension Damage vs. Strain

3.2. Material Properties of Steel

In the study by Jia & Kawamura [43], various steel material plasticity models applied in finite element (FE) analysis were evaluated and compared with experimental cyclic test results to identify the most suitable model for simulating cyclic behavior up to the onset of cracking in steel. The Chaboche model with isotropic hardening (IH) known as the combined hardening model, was found to predict monotonic and cyclic behavior in steel effectively [44]. The stress under cyclic loading with constant strain amplitude tended not to stabilize. This study employed the Chaboche model of SS400 steel, as shown in Table 1, because the planned material properties are similar to those used in this study. The combined hardening model is available in ABAQUS under the combined model options. The Mises yield function is further described by Equation 3.

$$dR = \mathrm{k}\,(Q_{\infty} - R)Q d\varepsilon_{eq} \quad (3)$$

where R and dR are change and incremental change in the size of the yield surface; and the initial value of R is zero, k is material parameter to describe the IH rate, and Q_{∞} is maximum change in the size of the yield surface.

Table 1. Material Properties of Plasticity Model of Steel [43]

Parameter	Chaboche Kinematic Hardening	Combined Hardening
σ_{y0}	255.9	255.9
C_1	97.2	26.9
C_2	97.2	1617.2
C_3	3,763.0	26.9
γ_1	0	0
γ_2	0	10.7
γ_3	13.7	0
k	-	5.7
$Q\infty$	-	227.8

3.3. Details of Connection and Geometry of Beam-Column Joint Models

The detailing of beam-column joint elements in the RC model, used as a benchmark in this study, followed the requirements of SNI-2847-2019 [45]. This detailing applied the concepts of strong column-weak beam and joint-weak column to ensure optimal structural behavior in accordance with seismic design principles. Meanwhile, the CS-01, CS-02, and CS-03 models were developed based on the RC model as a reference. These developments involved variations in several key parameters, such as reinforcement configuration, reinforcement ratio, and strength distribution, to evaluate the performance of the beam-column joint modifications under various loading conditions. This objective was to understand the impact of parameter changes on failure mechanisms, load capacity, and the ductile behavior of the structure. The results are expected to contribute to the design of more efficient and seismic-resistant beam-column joints. The details of the specimen models are presented in Table 2.

Overall, the variations in beam and column lengths and embedded steel configurations in each model were designed to enhance the performance of beam-column joints, particularly in terms of resistance to static and dynamic loads, including seismic forces. The joint model development details are shown in Figures 5. The detailing of beam-column joint elements in this study followed the concepts of strong column-weak beam and strong joint-weak column, aligned with the principles of seismic-resistant building structures utilizing a moment-resisting frame system. The column dimensions were 600 × 600 mm, and the beam dimensions were 400 × 600 mm. The concrete was designed to have a compressive strength of 30 MPa. Flexural reinforcement used deformed steel bars BjTS 420 (f_y=420 MPa, f_u=525 MPa), shear reinforcement uses plain steel BjTP 280 (f_y=280 MPa, f_u=350 MPa), and the steel quality is SS400 (f_y=250 MPa, f_u=400 MPa). The reinforcement details and embedded steel configurations are shown in Figure 6.

Table 2. Research Parameter of Beam Column Joint Models

Model	Research Parameter			
	Connection Type	Encased Steel Configuration	L Encased Steel in Beam (mm)	L Encased Steel in Column (mm)
RC	Monolithic	-	-	-
CS-01	Composite-Monolithic	Steel encased in concrete along the plastic hinge zones of both column and beam elements	1200	600
CS-02	Composite-Monolithic	Steel encased in the beam element along the plastic hinge zones and throughout the column element	1200	1682
CS-03	Composite-Monolithic	Steel encased throughout the beam and column elements to provide greater structural stability	2260	1682

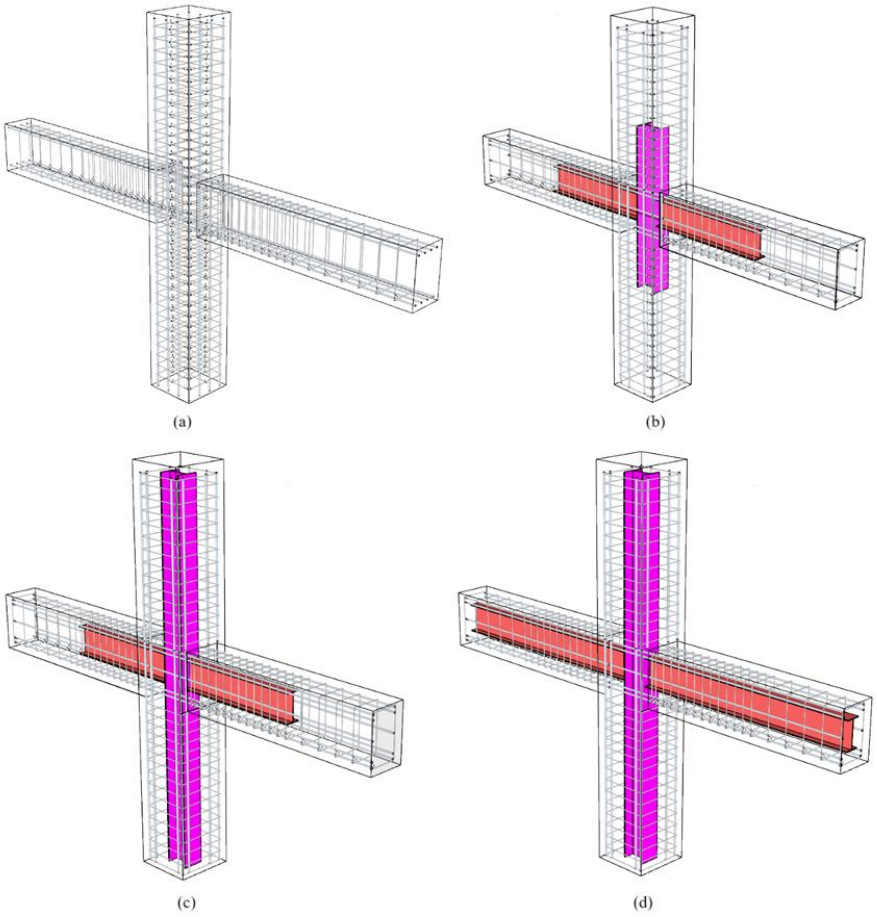

Figure 5. Details of Joint Model (a) RC (b) CS-01 (c) CS-02 (d) CS-03

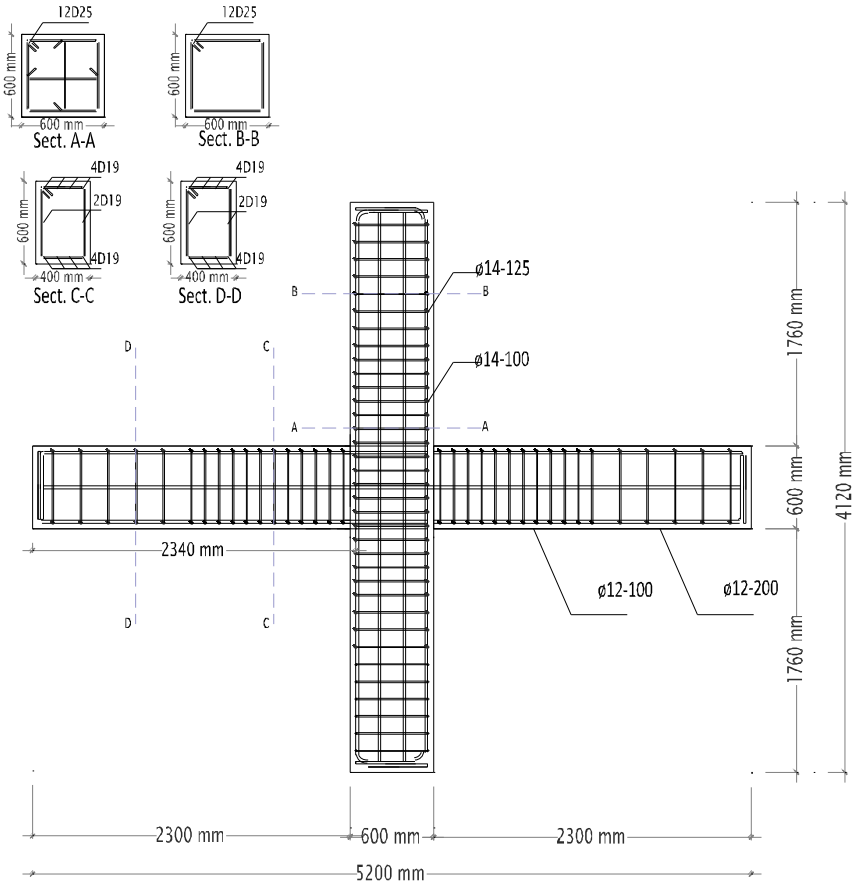

(a)

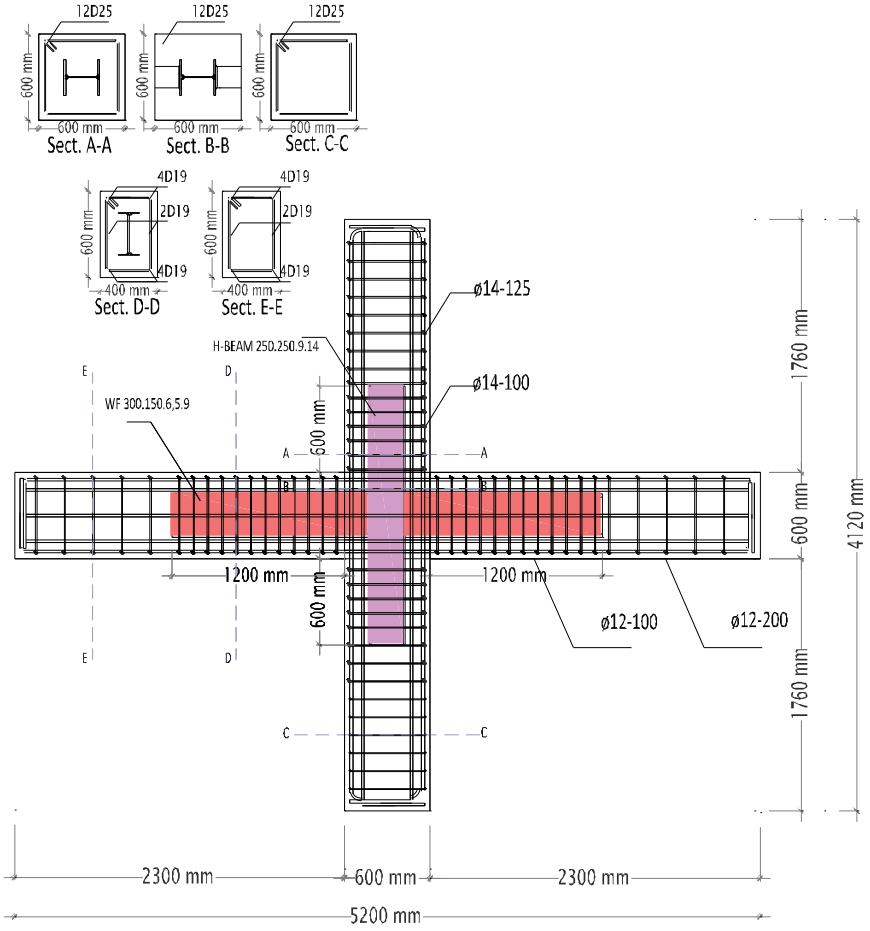
12D25
600 mm
Sect. A-A
Sect. B-B
Sect. C-C
4D19
2D19
400 mm
Sect. D-D
Sect. E-E
ø14-125
ø14-100
H-BEAM 250.250.9.14
WF 300.150.6.5.9
1200 mm
ø12-100
ø12-200
1760 mm
4120 mm
2300 mm
5200 mm

(b)

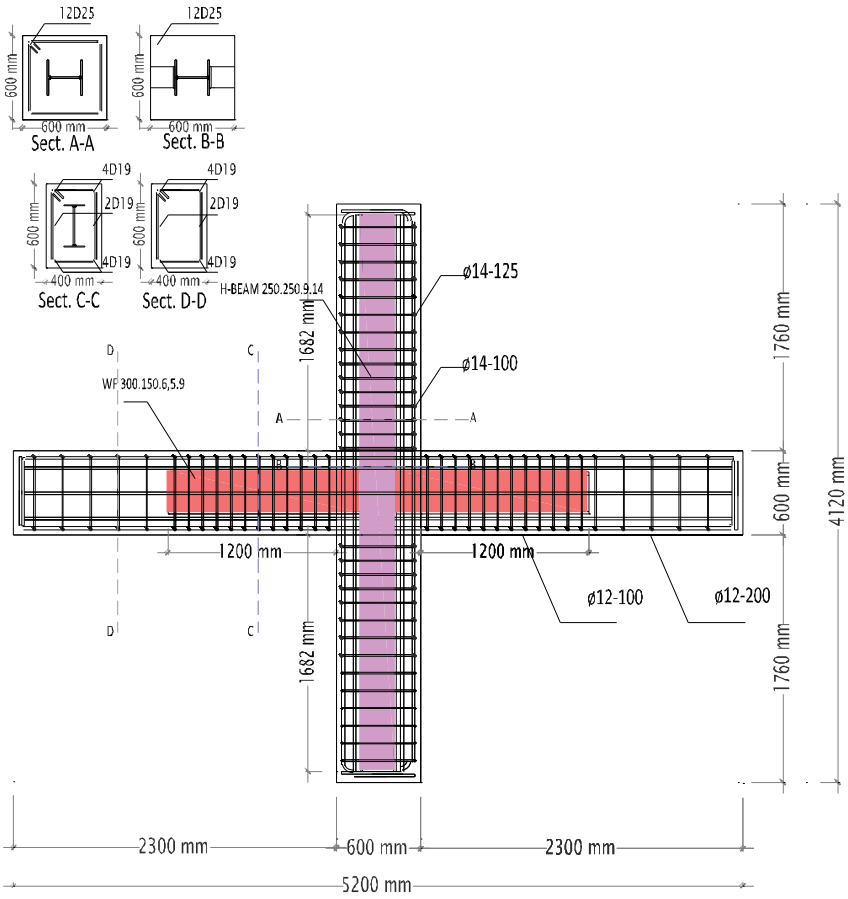
12D25
600 mm
Sect. A-A
Sect. B-B
4D19
2D19
400 mm
Sect. C-C
Sect. D-D
ø14-125
ø14-100
H-BEAM 250.250.9.14
WF 300.150.6.5.9
1682 mm
1200 mm
ø12-100
ø12-200
1760 mm
4120 mm
2300 mm
5200 mm

(c)

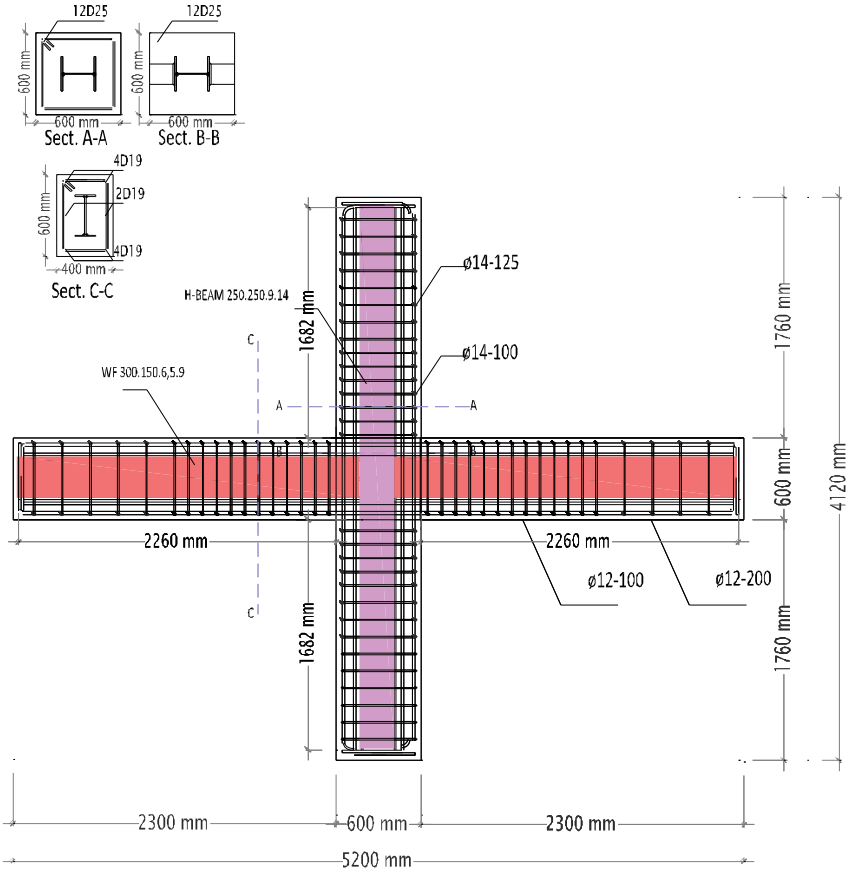

(d)

Figure 6. Detail of Reinforcement and Geometry of Beam-Column Joint: (a) RC (b) CS-01 (c) CS-02 (d) CS-03

3.4. Loading Configuration and Boundary Condition

This study analyzed interior beam-column joints under cyclic loading, following the ACI 374.2R-13 loading protocol [46], with a minimum drift ratio of 4%. Figure 7 illustrates the loading configuration and supports. According to ACI 374.2R-13 (2013), each deformation level must include a minimum of two loading cycles to ensure significant damage develops, with the number of cycles determined by the specified drift level. The selection of the number of cycles at each deformation level depends on the degradation characteristics of the system being tested, such as strength reduction, stiffness degradation, or energy dissipation. Figure 8 illustrates the loading history designed in accordance with the requirements of ACI 374.2R-13 (2013). This study applied cyclic loading using the column drift ratio parameter. The cyclic load was applied in two cycles for each deformation level, with a target drift ratio of 8%. The target displacement was determined using Equation 4. This approach was designed to simulate the response of beam-column joints under cyclic loading conditions resembling actual seismic scenarios, to provide a comprehensive understanding of structural performance, including deformation resistance, energy dissipation, and failure mechanisms.

$$\varphi n = 0.5 \text{ lc } (\varphi n) \tag{4}$$

where lc is column length, and φ is drift ratio.

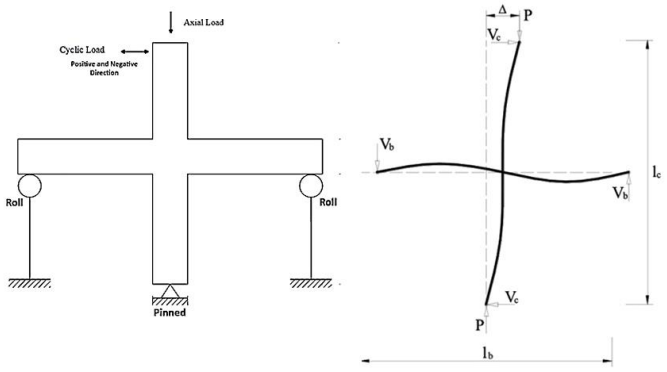

Figure 7. Loading Scheme of Modelling [32]

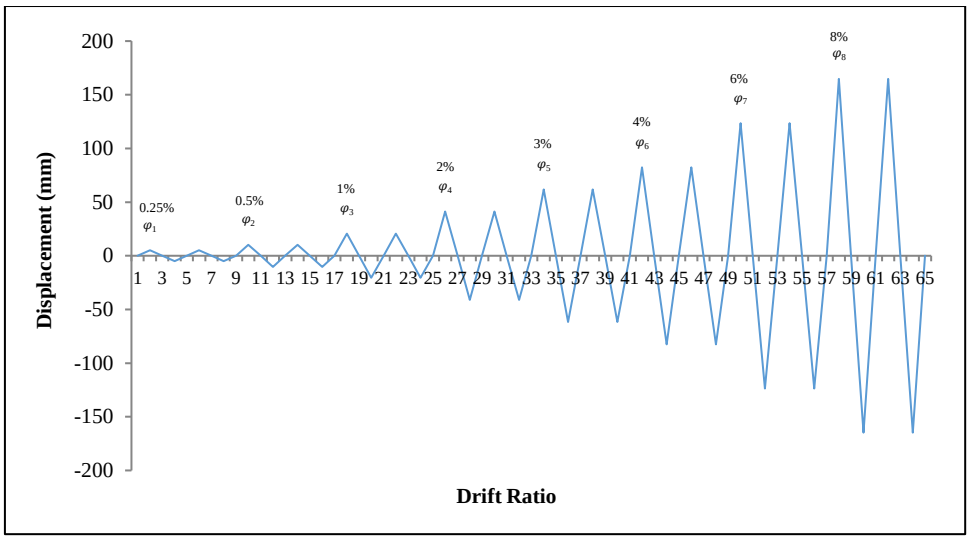

Figure 8. Cyclic Loading Procedure

3.5. Numerical Modelling using ABAQUS Software

ABAQUS is a comprehensive set of advanced engineering simulation tools that utilizes the finite element method to address a wide range of problems, from basic linear analyses to complex nonlinear simulations. In nonlinear analysis, ABAQUS automatically selects suitable load increments and convergence tolerances. During the modeling process, concrete reinforcement is represented by beam elements in ABAQUS, while the steel reinforcement is modeled with embedded elements and interaction connections. The detailed steps for modeling using the ABAQUS software are outlined in Figure 9, as shown below.

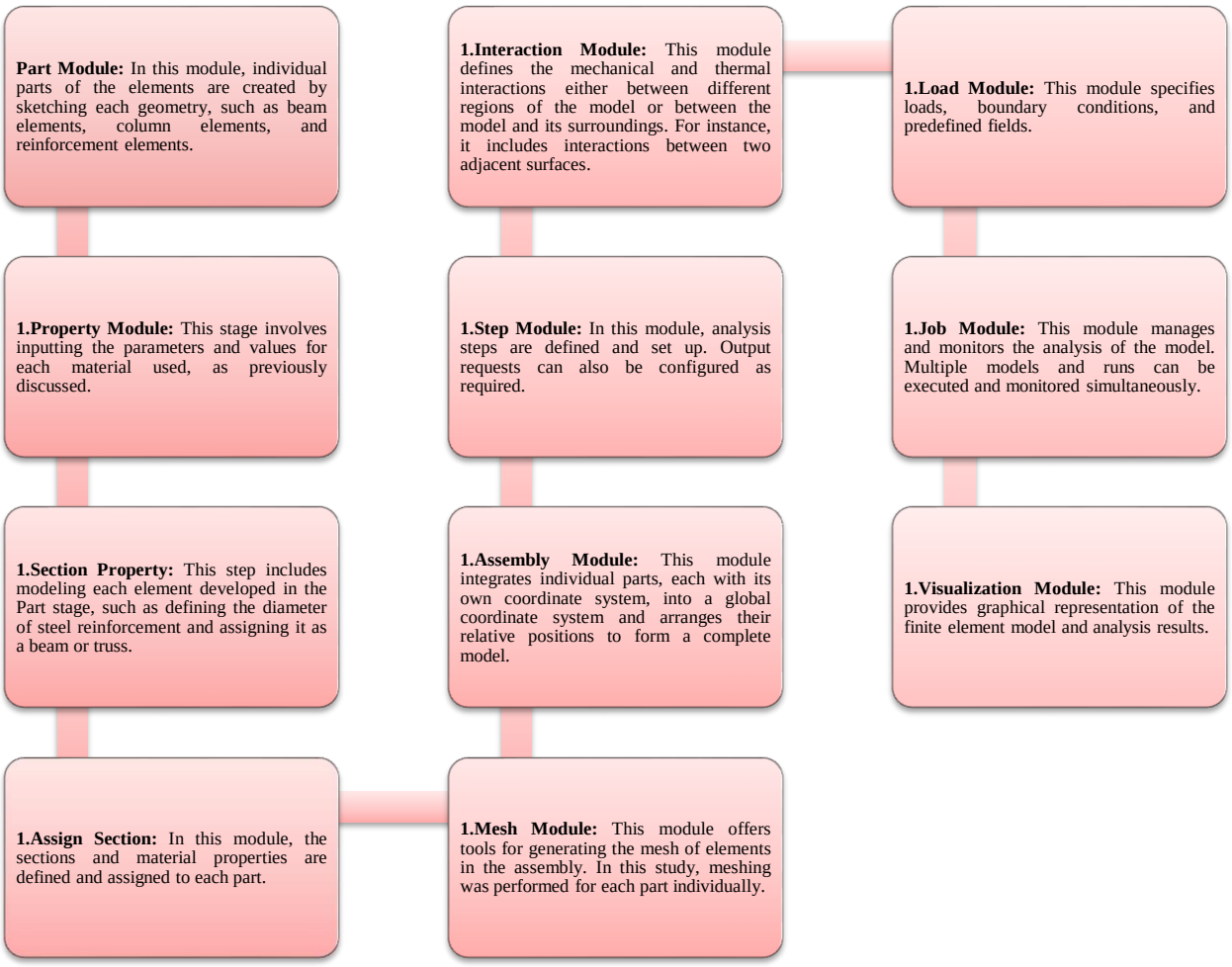

Figure 9. The steps for ABAQUS modelling

In ABAQUS modeling, various modules are used to define and analyze the structure. The Part Module is the first stage, where individual parts of the elements, such as beam, column, and reinforcement elements, are created by sketching their geometry. Following this, in the Property Module, material properties and parameters are defined for each material used, as previously discussed. The Section Property stage follows, where each element from the Part Module is modeled by defining specific attributes, such as the diameter of steel reinforcement, and assigning it a type, such as beam or truss. In the Assign Section Module, sections and material properties are assigned to each part. The Mesh Module is then used to generate meshes for each part individually, ensuring that the elements are discretized for analysis. In the Assembly Module, individual parts, each with its own coordinate system, are integrated into a global coordinate system, and their relative positions are arranged to create the complete model. Next, the Step Module used to define and configure analysis steps, as well as output requests if needed. The Interaction Module follows, defining the mechanical and thermal interactions between regions within the model or between the model and its surroundings, such as interactions between adjacent surfaces. In the Load Module, loads, boundary conditions, and predefined fields are specified to simulate real-world forces acting on the structure. The Job Module manages and monitors the analysis of the model, allowing multiple models and runs to be executed and observed simultaneously. Finally, the Visualization Module provides a graphical representation of the finite element model and the results from the analysis, enabling an easy interpretation of the structure's behavior under various conditions. Each module plays a crucial role in building, analyzing, and visualizing the model in ABAQUS.

4. Results and Discussion

An in-depth analysis of the structural performance of beam-column joints was conducted on four models: RC, CS-01, CS-02, and CS-03. This analysis aimed to evaluate the structural response of each model under a drift ratio of 8%. The axial load applied to the column in this analysis was 15% of the column capacity, representing actual load conditions that can occur in building structures. The analysis results included stress distribution, load-drift ratio relationships, energy dissipation, and moment-rotation relationships.

4.1. Stress Distribution

The structural element modeling of the beam-column joint produced comprehensive analytical data. One significant result was the stress distribution in the joint area, illustrating how stress was distributed and interacted with the structural elements. This stress distribution is visually presented in Figure 10, facilitating an understanding of the stress patterns and potential stress concentrations that may occur. These data are crucial for evaluating the joint's performance, particularly regarding capacity, stiffness, and potential structural failure under specific loading conditions.

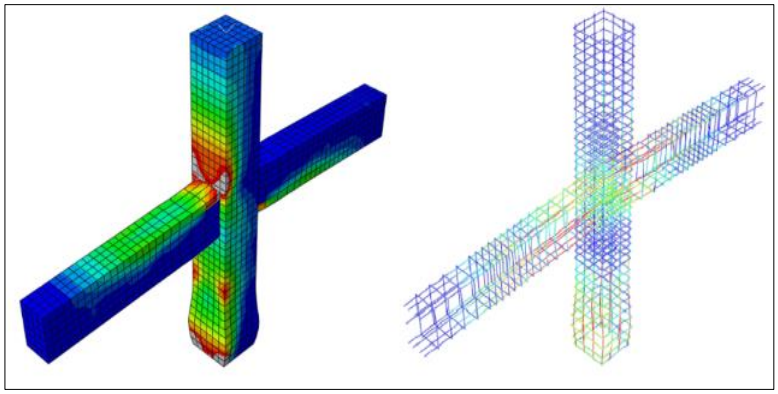

(a)

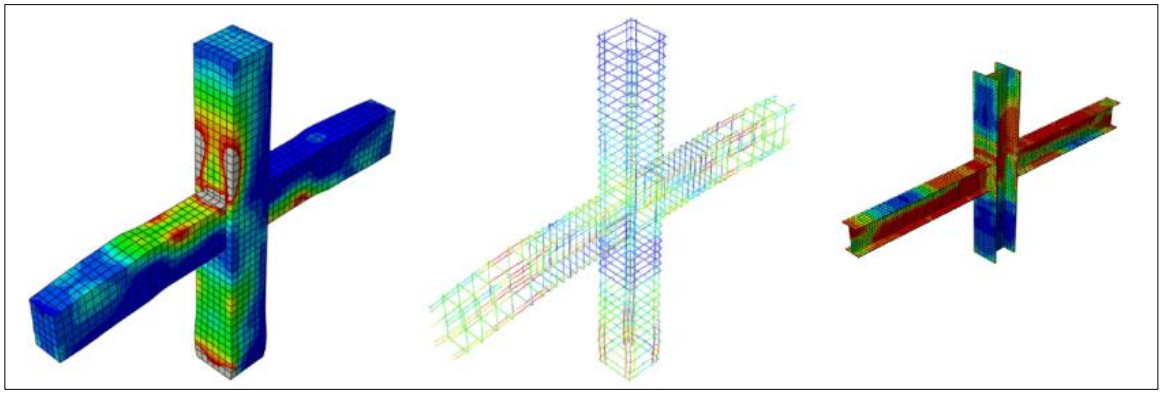

(b)

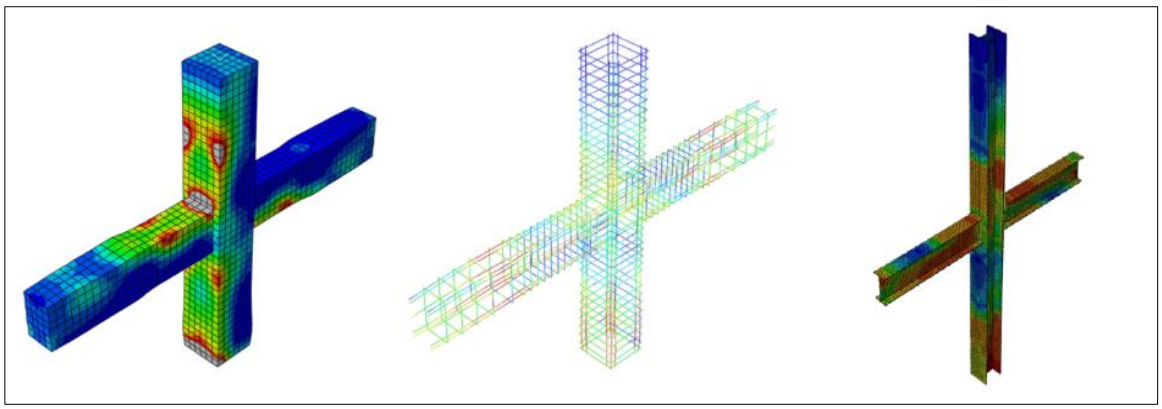

(c)

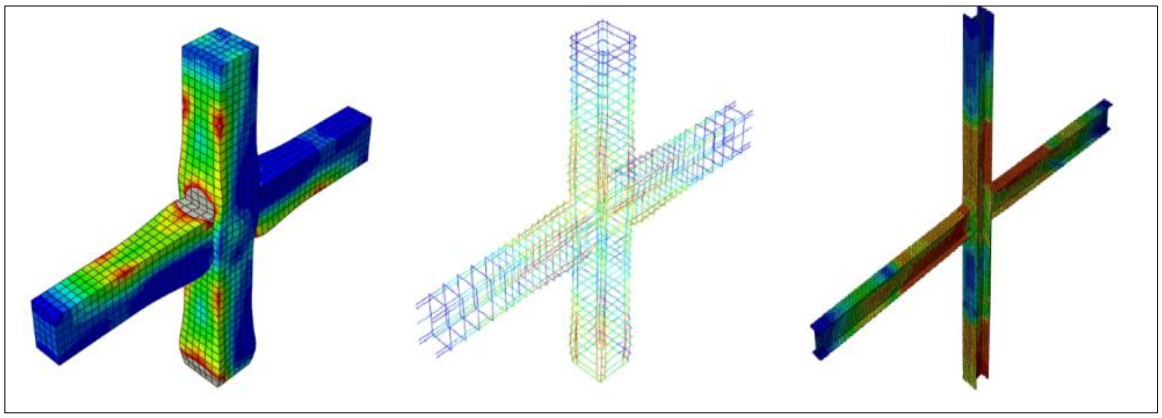

(d)

Figure 10. Stress Distribution of Model: (a) RC, (b) CS-01, (c) CS-02, (d) CS-03

Based on Figure 10, the highest stress in each model was located at the plastic hinge. The stress distribution displayed represents the model with axial load because the stress distribution in the model with zero axial load was not significantly different, likely due to the relatively small axial load applied. However, in the RC model, the highest stress was found in the beam reinforcement at the face of the column, while in the CS-01, CS-02, and CS-03 models, the highest stress was concentrated in the steel elements within the plastic hinge area. A comparison of the results also indicated that the stresses in the concrete elements of models CS-01, CS-02, and CS-03 were more evenly distributed. This demonstrated that the steel within the concrete can absorb the applied energy, thereby reducing the stresses in both the reinforcement and the concrete. The comparison between models CS-01, CS-02, and CS-03 appeared in the magnitude of stress occurring in the steel elements. In model CS-01, the highest stress was observed based on the contour colors from the finite element analysis (with the stress distribution contour scaled). In contrast, the steel elements in models CS-02 and CS-03, which had longer element lengths, showed a smaller stress distribution. For model CS-03, where the steel elements fully spanned both the beams and columns, significant stress occurred in the reinforcement within the plastic hinge areas. Therefore, based on the stress distribution analysis, model CS-02 demonstrated the best performance.

4.2. Lateral Load-Drift Ratio Relationships

The analysis included a comparison of structural performance between models subjected to pure cyclic loading and those with a combination of axial loading. This evaluation aimed to understand the impact of axial load variations on the structural response, particularly in beam-column joints. Figures 11 present the load-drift ratio curves of the models under cyclic and axial load, illustrating the structural behavior in resisting lateral deformations under various loading conditions. Meanwhile, Figure 12 shows backbone curves, specifically comparing the performance of models under axial loads of 0 $f'c\ A_g$ and 0.15 $f'c\ A_g$ of the column capacity. From these backbone curves, differences in capacity and the structure's ability to absorb energy under different loading conditions can be analyzed. The results demonstrated the role of axial loading in enhancing or reducing the performance of structural elements, which is a critical aspect in the design of beam-column joints for seismic-resistant structures or other loading conditions.

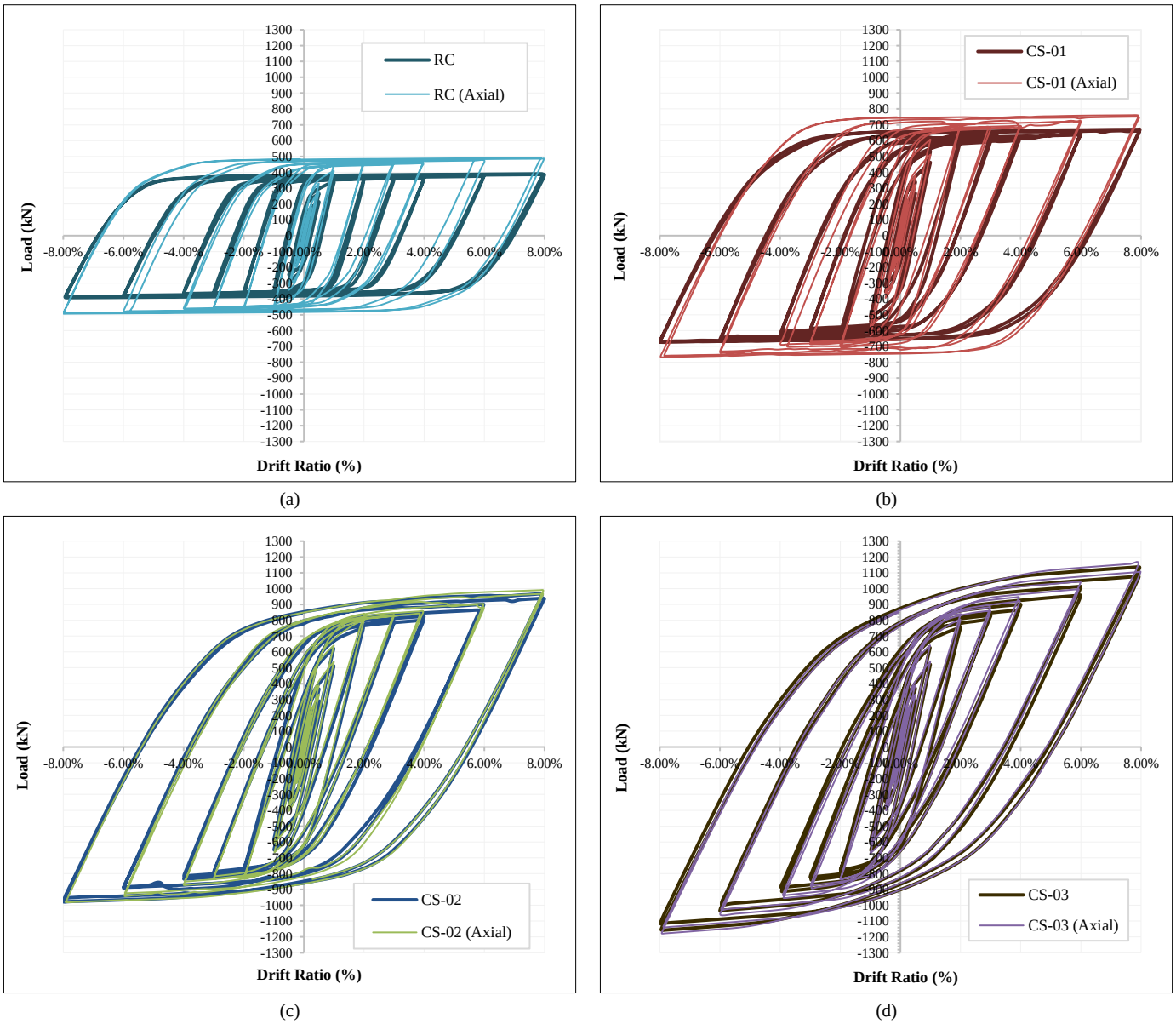

Figure 11. Load-Drift Ratio Hysteresis Curve: (a) RC, (b) CS-01, (c) CS-02, (d) CS-03

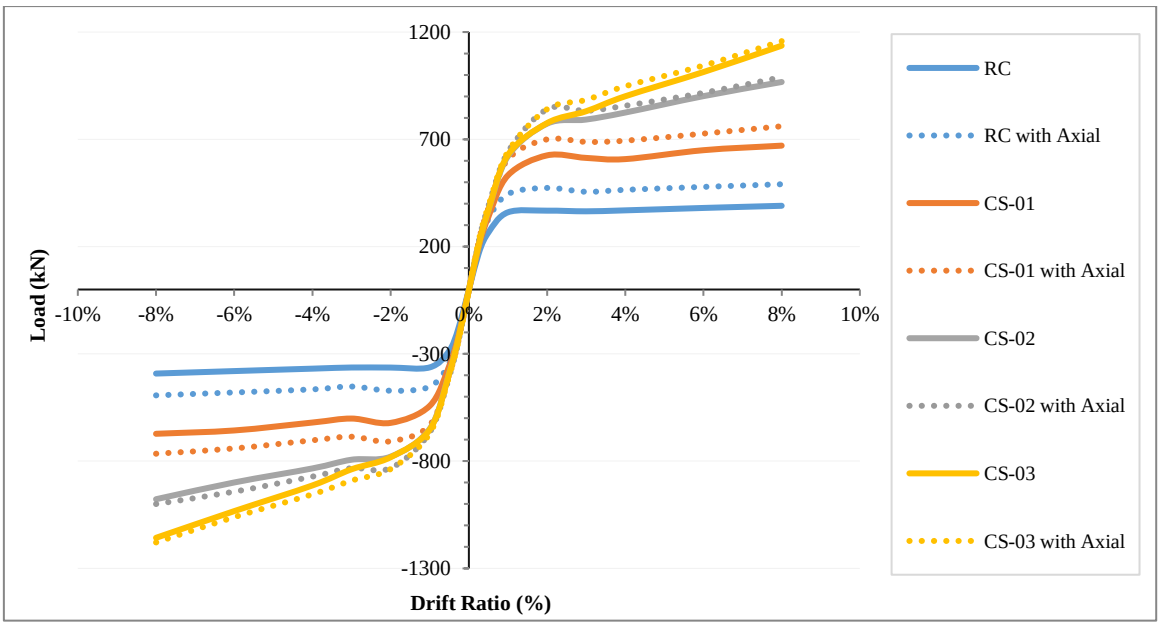

Figure 12. Backbone Curve of The Models

Table 3 presents a comparative analysis of the structural capacity of beam-column joints between the RC and CS models, showing a trend of increased capacity when subjected to an axial load (0.15 $f'c\ A_g$) compared to the condition without axial load (0). Table 3 indicates that the RC model had a lower load capacity compared to the CS models. The CS-03 model exhibited the highest load capacity, particularly in the negative direction, reaching 1157.42 kN (2.95 times greater than the RC model). The influence of steel elements on load capacity was substantial. The more steel elements applied, the greater the resulting load capacity. This was evident from the load capacity results of the CS-01 model in the negative direction with an 8% drift ratio, reaching 672.535 kN. The CS-02 model showed an increase in capacity to 977.426 kN (45% greater than CS-01), while the CS-03 model reached 1157.42 kN (18% greater than CS-02). In addition, the effect of the applied axial load, which was 0.15 $f'c\ Ag$ increased the load capacity in all models. For example, in the RC model in the positive direction with an 8% drift ratio, the load capacity increased to 490.696 kN (25% compared to the condition without axial load). The CS-01 model showed an increase of 13%, while CS-02 and CS-03 increased by 2% and 1.8%, respectively. These results indicated that the greater the amount of steel in the concrete, the smaller the effect of axial load on overall load capacity. This suggests that steel elements enhance load capacity and reduce the structural sensitivity to axial load variations. The CS models demonstrated significant advantages over the RC model, emphasizing the role of steel elements in enhancing structural capacity and performance against lateral deformations. Combined with the visualization in the backbone curves (Figure 12), these data provide a comprehensive understanding of the structural response of joints under cyclic and axial loading conditions, a critical aspect in designing seismic-resistant structures.

Table 3. Load-Drift Ratio Value of Each Models

Drift Ratio	Load (kN)							
	RC	RC With Axial	CS-01	CS-01 With Axial	CS-02	CS-02 With Axial	CS-03	CS-03 With Axial
-8%	-391.811	-493.306	-672.535	-765.372	-977.426	-999.852	-1157.42	-1178.91
-6%	-380.211	-479.773	-656.964	-740.735	-899.371	-942.333	-1032.92	-1060.92
-4%	-368.919	-465.572	-620.052	-702.892	-833.907	-871.981	-913.142	-954.748
-3%	-363.531	-452.25	-601.535	-686.198	-793.346	-832.59	-837.938	-890.634
-2%	-363.831	-471.725	-621.6	-707.4	-779.036	-832.591	-781.612	-836.726
-1%	-362.996	-452.933	-542.22	-631.716	-649.361	-665.417	-652.461	-671.188
-0.50%	-285.502	-342.723	-355.387	-393.541	-385.662	-405.097	-389.755	-401.386
-0.25%	-171.028	-199.426	-204.223	-226.526	-213.078	-228.654	-214.687	-230.304
0.25%	167.304	196.339	198.007	222.101	206.831	222.957	207.786	226.307
0.50%	265.748	328.711	339.152	379.324	365.958	388.927	369.63	388.309
1%	359.879	444.972	532.265	607.149	621.556	641.288	627.361	642.391
2%	367.393	473.442	625.165	699.86	772.925	840.047	775.46	840.343
3%	364.445	455.518	613.359	688.235	792.129	832.969	830.905	883.896
4%	368.926	464.651	607.737	693.609	824.8	856.552	900.611	947.528
6%	380.096	478.351	649.331	726.665	901.337	916.635	1013.54	1043.94
8%	390.146	490.696	670.545	760.968	967.162	989.971	1136.51	1157.61

Overall, the results demonstrated that steel reinforcement significantly improves the structural performance of beam-column joints, especially in terms of load capacity. The CS model, which incorporated varying amounts of steel, show marked improvements over the RC model, with the CS-03 model demonstrating the best capacity. The axial load enhanced the load capacity in the RC model but had a reducing effect in the SRC models, which indicated that the higher the steel content in the structure, the less sensitive it became to changes in axial load. This finding is crucial in seismic-resistant design, where structures need to absorb and dissipate energy efficiently while maintaining stability under both lateral and axial loading conditions. The increased capacity of SRC models, especially when axial load is applied, highlights the critical role of steel elements in ensuring structural integrity during seismic events. A comparison can be made with the previous study conducted by Sermet et al. (2021) [8], in which the S1 model used in their research showed a similar configuration to the CS-02 model in this study. Both models incorporate steel reinforcement and are designed to assess the performance of beam-column joints under cyclic loading. However, one notable difference is that the study by Sermet et al. (2021) [8] did not address or explain the effects of applying axial loads on the performance of these models. By including axial load considerations, this study aims to fill the gap left by Sermet et al. (2021) [8], providing a more comprehensive analysis of how axial loads interact with cyclic loading to affect the overall performance and stability of steel-reinforced concrete beam-column joints.

4.3. Energy Dissipation Capacity

Energy dissipation refers to the amount of energy that a structure can absorb and release before it loses stability and collapses during a seismic event. Therefore, the ability of beam-column joints to dissipate energy is one of the key parameters in evaluating the performance of a structure during seismic events. The comparison of four beam-column joint models, with and without the influence of axial loads, is presented in Table 4 and Figure 13

Table 4. Energy Dissipation each of model

Model	Energy Dissipation Capacity (kNm)	The comparison between with axial load and zero axial load	The comparison between the development model and the control model
RC	935.487	9.34%	-
RC (Axial)	1022.84		-
CS-01	1317.39	-2.99%	40.82%
CS-01 (Axial)	1278.01		24.95%
CS-02	1395.22	-2.88%	49.14%
CS-02 (Axial)	1355.07		32.48%
CS-03	1312.42	-2.09%	40.29%
CS-03 (Axial)	1284.95		25.63%

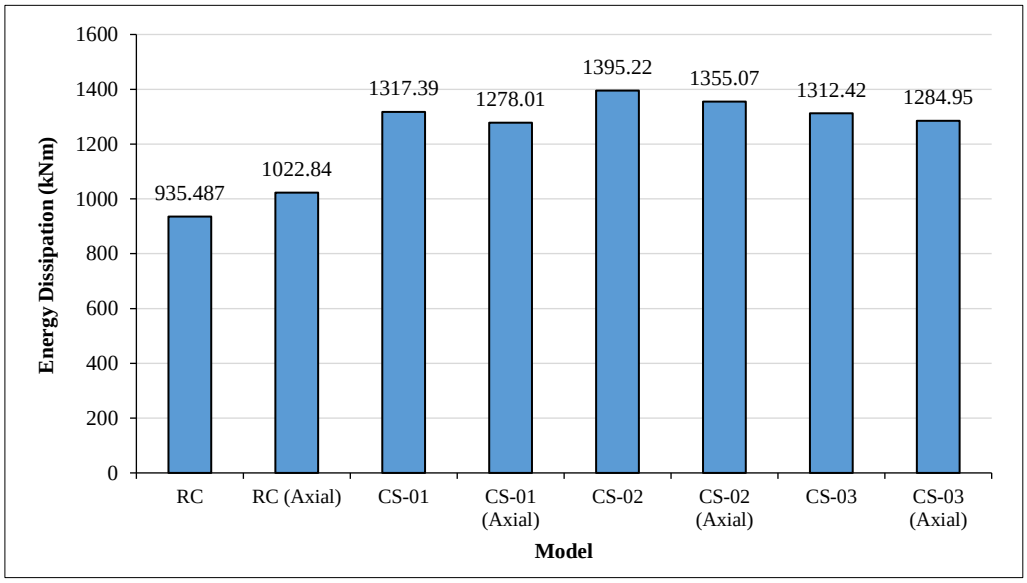

Figure 13. Energy Dissipation Capacity

The analysis of energy dissipation capacity indicated that generally SRC beam-column joint models exhibit high energy dissipation capacities compared to the RC model. The CS-01 model achieved an energy dissipation capacity of 1317.39 kNm, 40.82% higher than the RC model. The CS-02 model showed an increase of 49.14%, while the CS-03 model had an energy dissipation capacity 40.29% greater than the RC model. However, the effect of axial load on each model produced differing results. In the RC model, applying axial load enhanced the energy dissipation capacity. Conversely, in models with steel reinforcement (SRC), namely CS-01, CS-02, and CS-03, the energy dissipation capacity was slightly lower than the case without axial load. The CS-01 model experienced a reduction in energy dissipation capacity by 2.99%, while CS-02 and CS-03 by 2.88% and 2.09%, respectively. These findings demonstrated that the influence of axial load on energy dissipation depends significantly on each model's design and structural configuration. Overall, this analysis suggested that axial load positively contributes to increasing energy dissipation capacity in the RC model. In terms of structural design, these changes are generally within acceptable limits. The reductions in energy dissipation under axial load are minor and do not drastically impact the overall performance of the structure, particularly in comparison to the benefits provided by the higher steel reinforcement in the SRC models. The slight reduction suggests that while axial load can slightly reduce the effectiveness of the steel elements in energy dissipation, the overall structural stability and performance are not significantly compromised. Therefore, the changes in energy dissipation caused by axial load are acceptable for structural design purposes, particularly for structures in seismic-prone areas where ensuring sufficient energy dissipation is crucial. The benefits of increased steel reinforcement in the SRC models, which provide higher energy dissipation capacity compared to the RC model, still outweigh the slight reductions observed under axial load, making these models suitable for use in seismic-resistant design.

However, in SRC models, although the overall energy dissipation capacity remains higher than that of RC models, applying axial load causes a slight reduction in energy dissipation capacity. This is attributed to the contribution of steel elements in reinforcing the concrete, which enhances the structure's ability to absorb energy from cyclic loading but becomes less effective under axial load. These results highlight the importance of considering structural design and configuration when evaluating the performance of beam-column joints, particularly under conditions with and without axial load. Axial load enhances energy dissipation in the RC model but slightly reduces it in the SRC models due to the distinct roles that axial load plays in the behavior of reinforced concrete (RC) structures versus steel-reinforced concrete (SRC) structures. In the RC model, the application of axial load leads to improved energy dissipation. This is because axial load compresses the concrete, enhancing its ability to resist forces and absorb energy, especially under cyclic loading conditions typical of seismic events. The axial load helps in compacting the concrete, making it more effective at dissipating energy through the friction and internal resistance generated within the concrete mass. Therefore, the presence of axial load in the RC model increases its overall energy dissipation capacity. However, in the SRC models (CS-01, CS-02, and CS-03), the influence of axial load is different. These models already have a substantial amount of steel reinforcement, which helps the concrete absorb and dissipate energy from seismic forces. When axial load is applied to these SRC models, it results in compressive forces on the steel reinforcement, which can reduce the steel's efficiency in contributing to energy dissipation. The steel reinforcement, which is effective in absorbing energy from cyclic loading, becomes less effective under the additional axial load. This reduction in the effectiveness of the steel reinforcement leads to a slight decrease in energy dissipation capacity in the SRC models when axial load is applied. In summary, axial load enhances energy dissipation in the RC model by improving the compression of concrete, making it more effective at energy absorption. In contrast, in SRC models, although the overall energy dissipation remains higher than in the RC model, axial load slightly reduces the capacity due to the reduced efficiency of the steel reinforcement under compression.

4.4. Moment-Rotation Relationships

The moment-rotation data presented in Table 5 were used to evaluate the performance of beam-column joint models in the ABAQUS program under various conditions, focusing on their maximum bending moment capacities, rotations, and failure criteria based on the ACI 374.2R-13 standards. The results of this rotation analysis can be utilized to determine the structural performance level, which serves as a basis for setting deformation limits for elements and components at each performance level. In this study, the plastic rotation values were obtained from the displacement at the beam element point at the column face and then processed and analyzed to derive the plastic hinge rotation values in radians. Subsequently, these results were classified according to ACI PRC-374.2-13 standards to establish the performance level criteria for the structural elements.

Table 5. Moment-Rotation Relationship

Model	Load Direction	Moment (kNm)	Rotation (Rad)	Performance Level Criteria (ACI PRC-374.2-13)
RC	Positive	687	0.0230	Life Safety
	Negative	-690		
RC (Axial)	Positive	864	0.0335	Collapse Prevention
	Negative	-868		
CS-01	Positive	1180	0.0266	Collapse Prevention
	Negative	-1184		
CS-01 (Axial)	Positive	1339	0.0304	Collapse Prevention
	Negative	-1347		
CS-02	Positive	1702	0.0303	Collapse Prevention
	Negative	-1720		
CS-02 (Axial)	Positive	1742	0.0306	Collapse Prevention
	Negative	-1726		
CS-03	Positive	2000	0.0235	Life Safety
	Negative	-2037		
CS-03 (Axial)	Positive	2037	0.0236	Life Safety
	Negative	-2075		

Table 5 presents the moment-rotation relationship for various beam-column joint models tested using a structural analysis program, considering the load direction (positive and negative) and performance level criteria based on ACI 374.2R-13. The moment magnitude is directly proportional to the load capacity, as explained in the load-drift ratio results. Based on this, the conclusions regarding the moments are similar, focusing on the rotation values measured in radians. The analysis showed that the RC model (without axial load) and the CS-03 model met the 'Life Safety' performance level criteria. In contrast, the other models met the 'Collapse Prevention' performance level criteria. A 'Life Safety' model can ensure occupant protection despite significant damage, while a 'Collapse Prevention' model can prevent collapse but may let more severe damage to occur. These results revealed that although the CS-03 model performed the best in terms of load capacity and energy dissipation compared to the RC, CS-01, and CS-02 models, its rotation value tended to be smaller and fell into the 'Life Safety' performance level. The CS-03 model, despite having the highest load capacity, exhibited lower plastic rotation compared to the CS-01 and CS-02 models due to its more extensive use of steel encasement in both the beam and column elements. According to the research parameters, the CS-03 model had the longest steel encasement in the beam (2260 mm) and the same length in the column (1682 mm) as the CS-02 model. This greater encasement in the beam element of CS-03 enhanced its structural stability and stiffness, which resulted in a higher load capacity. However, increased stiffness typically leads to lower plastic rotation capacity.

The classification of the CS-03 model under the 'Life Safety' performance level in practical seismic design applications has several important implications. Firstly, it indicates that while the structure may experience significant damage during an earthquake, it will still be able to protect its occupants. Even in the event of severe seismic forces, the structure prevents life-threatening hazards, ensuring the safety of individuals inside the building. Secondly, the 'Life Safety' classification suggests that the building can still be evacuated safely, and repairs can be made afterward, as the overall structural integrity will be maintained despite the damage. This classification also emphasizes the importance of designing structures that can withstand significant seismic activity while safeguarding human life. It helps engineers balance safety, cost, and performance requirements in seismic regions. Conversely, the CS-01 and CS-02 models, falling under the 'Collapse Prevention' performance level, were more suitable for application in seismic areas. This classification in practical seismic design applications has several important implications. These models are designed to prevent the structural collapse during a seismic event, even if the structure experiences significant damage. This means that the primary objective is to ensure that the building does not fully collapse, which could potentially lead to catastrophic consequences such as the loss of life and destruction of property. The 'Collapse Prevention' performance level suggests that while these models can prevent collapse, they may still experience severe damage, such as cracking or deformation, that could affect the building's usability or aesthetic appeal.

In practical terms, this could mean that the building may require extensive repairs after an earthquake but will not be in danger of total failure. Finally, the CS-01 and CS-02 models' classification under this level highlights the importance of designing buildings that can withstand major seismic events while ensuring the building's ability to prevent total collapse, minimizing the risk to occupants and reducing potential for catastrophic failure. The finding that the CS-02 model provides the best seismic performance in this study is likely specific to the tested configurations and may not be directly applicable to all types of structures. The results depend on the specific design and configuration of the beam-column joint models used in the study, which were designed with varying encasement in the beam and column elements. In the case of the CS-02 model, the steel encasement in both the beam and column provides a balance between energy dissipation and load capacity, making it particularly effective for the tested configuration. However, the seismic performance of a structure is influenced by various factors, including the type of building, the materials used, the structural design, and the specific loading conditions. Different structures may have unique requirements depending on their purpose, location, and exposure to seismic forces. In addition, the CS-02 model's performance is closely linked to its structural configuration (e.g., steel encasement in the beam and column). This configuration might not be suitable for all types of structures, especially those with different load-bearing requirements or materials. Thus, while the CS-02 model proves effective for the specific beam-column joint configurations tested in this study, its performance cannot be universally generalized. This study's findings should be interpreted in the context of the tested configurations, and the seismic performance of other types of structures would need to be evaluated based on their unique characteristics and design requirements.

5. Conclusions

The research findings provided an in-depth evaluation of the structural performance of beam-column joints under cyclic and axial loading conditions for four models: RC, CS-01, CS-02, and CS-03. The analysis focused on stress distribution, load-drift ratio relationships, energy dissipation capacity, and moment-rotation relationships, revealing the critical role of axial load and steel-reinforced concrete in the structural performance of the beam-column joints.

- The stress distribution analysis of the beam-column joint models revealed significant findings regarding stress patterns and potential concentrations. The highest stress in each model was located at the plastic hinge, with the RC model showing the highest stress at the beam reinforcement at the column face. In contrast, models CS-01, CS-02, and CS-03 showed stress concentrations in the steel elements within the plastic hinge area. The comparison indicated that including steel elements in concrete helps distribute stresses more evenly, absorbing applied energy and reducing stress in reinforcement and concrete.

- Axial load significantly influenced the structural performance of beam-column joints, particularly in models subjected to cyclic loading. The CS models outperform the RC model in load capacity, with CS-03 showing the highest load capacity, especially under axial load conditions. Steel elements in the models enhanced load capacity and reduced the structure's sensitivity to variations in axial load. The results emphasized the importance of incorporating steel elements in the design of seismic-resistant structures, as they improve performance under both lateral deformations and axial loading conditions.
- Development of beam-column joint models, particularly those with steel reinforcement (SRC), exhibited higher energy dissipation capacities compared to the RC model. While axial load enhanced energy dissipation in the RC model, it slightly reduced the dissipation capacity in the SRC models. The presence of steel elements improved the overall energy dissipation but became less effective under axial load. These findings emphasized the significance of structural design and configuration in evaluating the performance of beam-column joints, especially under varying loading conditions.
- Moment-rotation data indicated that the RC and CS-03 models met the 'Life Safety' performance criteria, while the other models meet 'Collapse Prevention.' While the CS-03 model excelled in load capacity and energy dissipation, its rotation value placed it in the 'Life Safety' category. In contrast, the CS-01 and CS-02 models demonstrated better performance for seismic-prone areas, qualifying for the 'Collapse Prevention' level. These findings highlighted the importance of rotation and load capacity in determining the structural performance and suitability for different seismic conditions.

Overall, the analysis results indicated that the CS-03 model performed the best compared to the RC, CS-01, and CS-02 models in terms of load capacity and energy dissipation. However, this model showed a lower plastic rotation result, categorizing it under the 'Life Safety' performance level. The results revealed that the CS-02 model exhibited the best and most effective seismic performance compared to the other models. Regarding the effect of axial load, there were variations in its impact across each model, but the trend of the results remained similar. The axial load effect could increase the load capacity in all models. Regarding energy dissipation, the axial load effect increased the capacity in the RC model. In contrast, in the CS models, the application of axial load slightly reduced energy dissipation capacity, although the results were not significant. Meanwhile, the effect of axial load on rotation varied across the models

6. Declarations

6.1. Author Contributions

Conceptualization, D.I. and B.S.; methodology, B.S., A.R.A., and Y.T.; software, D.I. and Y.S.; validation, Y.S., D.I., and Y.S.; formal analysis, B.S.; investigation, D.I.; resources, D.I.; data curation, D.I.; writing—original draft preparation, Y.S.; writing—review and editing, Y.T.; visualization, D.I.; supervision, A.R.A.; project administration, B.S.; funding acquisition, D.I. All authors have read and agreed to the published version of the manuscript.

6.2. Data Availability Statement

The data presented in this study are available in the article.

6.3. Funding

The authors received no financial support for the research, authorship, and/or publication of this article.

6.4. Conflicts of Interest

The authors declare no conflict of interest.

7. References

[1] Hai, L., Luo, J., Yang, L., & Ban, H. (2022). Experimental study on monotonic and cyclic behaviour of deconstructable beam-to-column composite joints. Engineering Structures, 272(April), 114990. doi:10.1016/j.engstruct.2022.114990.

[2] Mostafa, M. M. A., Wu, T., Liu, X., & Fu, B. (2019). The Composite Steel Reinforced Concrete Column Under Axial and Seismic Loads: A Review. International Journal of Steel Structures, 19(6), 1969–1987. doi:10.1007/s13296-019-00257-9.

[3] Le, D. D., Nguyen, X. H., & Nguyen, Q. H. (2020). Cyclic testing of a composite joint between a reinforced concrete column and a steel beam. Applied Sciences (Switzerland), 10(7), 2385. doi:10.3390/app10072385.

[4] Shehab, B. A., & Ekmekyapar, T. (2021). Joints behaviour of through steel beam to composite column connection: Experimental study. Marine Structures, 76(December), 102921. doi:10.1016/j.marstruc.2020.102921.

[5] Kuramoto, H., Li, B., Meas, K., & Fauzan. (2011). Experimental and Analytical Performance Evaluation of Engineering Wood Encased Concrete-Steel Beam-Column Joints. Journal of Structural Engineering, 137(8), 822–833. doi:10.1061/(asce)st.1943-541x.0000334.

[6] Wu, C., Liu, J., Tan, W., & Wang, P. (2020). Seismic behavior of composite interior joints of prefabricated H-shaped steel reinforced concrete column - steel beam. Structures, 23, 558–572. doi:10.1016/j.istruc.2019.11.008.

[7] Djamaluddin, R., Irmawaty, R., & Yamaguchi, K. (2024). Flexural Behavior of Repaired Reinforced Concrete Beams Due to Corrosion of Steel Reinforcement Using Grouting and FRP Sheet Strengthening. Civil Engineering Journal, 10(1), 222-233. doi:10.28991/CEJ-2024-010-01-014.

[8] Şermet, F., Ercan, E., Hökelekli, E., Demir, A., & Arısoy, B. (2021). The behavior of concrete-encased steel composite column-beam joints under cyclic loading. Structural Design of Tall and Special Buildings, 30(6), 1–20. doi:10.1002/tal.1842.

[9] Shaaban, I. G., & Said, M. (2018). Finite element modeling of exterior beam-column joints strengthened by ferrocement under cyclic loading. Case Studies in Construction Materials, 8, 333–346. doi:10.1016/j.cscm.2018.02.010.

[10] Chen, L., Feng, J., Xue, Y., & Liang, C. (2023). Seismic behavior of an innovative prefabricated steel-concrete composite beam-column joint. Journal of Building Engineering, 76(March), 107211. doi:10.1016/j.jobe.2023.107211.

[11] Venkatesan, B., Ilangovan, R., Jayabalan, P., Mahendran, N., & Sakthieswaran, N. (2016). Finite Element Analysis (FEA) for the Beam-Column Joint Subjected to Cyclic Loading Was Performed Using ANSYS. Circuits and Systems, 7(8), 1581–1597. doi:10.4236/cs.2016.78138.

[12] Asran, A., Al-Esnawy, H., & Fayed, S. (2016). A review on reinforced concrete beam-column connections. In The International Conference on Civil and Architecture Engineering, International Conference on Civil and Architecture Engineering, 1-27. doi:10.21608/iccae.2016.43415.

[13] Kotwal, S. S., Kadam, V. S., More, M. M., Patil, A. S., & Mohite, N. A. (2022). A Literature Review on Beam Column Joints with Different Loading Condition and Methods of Strengthening. International Journal for Research in Applied Science and Engineering Technology, 10(5), 4017–4022. doi:10.22214/ijraset.2022.43318.

[14] Septiarsilia, Y., Iranata, D., & Suswanto, B. (2023). Hybrid Beam-Column Connection of Precast Concrete Structures: A Review. E3S Web of Conferences, 434, 1–12. doi:10.1051/e3sconf/202343402019.

[15] Ghayeb, H. H., Razak, H. A., & Sulong, N. H. R. (2017). Development and testing of hybrid precast concrete beam-to-column connections under cyclic loading. Construction and Building Materials, 151, 258–278. doi:10.1016/j.conbuildmat.2017.06.073.

[16] Fan, J. J., Wu, G., Feng, D. C., Zeng, Y. H., & Lu, Y. (2020). Seismic performance of a novel self-sustaining beam-column connection for precast concrete moment-resisting frames. Engineering Structures, 222(June), 111096. doi:10.1016/j.engstruct.2020.111096.

[17] Septiarsilia, Y., Iranata, D., Suswanto, B. (2024). Evaluation of Beam–Column Connection Capacity According to SNI 2847–2019 and SNI 1726–2019. Advances in Civil Engineering Materials. ICACE 2023, Lecture Notes in Civil Engineering, 466, Springer, Singapore. doi:10.1007/978-981-97-0751-5_82.

[18] Yang, X., Dong, Y., Liu, X., Qiu, T., & Zhou, J. (2024). Seismic Behavior of Concrete Beam-Column Joints Reinforced with Steel-Jacketed Grouting. Buildings, 14(10). doi:10.3390/buildings14103239.

[19] Zhang, L., Yao, J., Hu, Y., Gao, J., & Cheng, Z. (2022). Predicting shear strength of steel fiber reinforced concrete beam-column joints by modified compression field theory. Structures, 41, 1432–1441. doi:10.1016/j.istruc.2022.05.072.

[20] Gou, S., Ding, R., Fan, J., Nie, X., & Zhang, J. (2019). Experimental study on seismic performance of precast LSECC/RC composite joints with U-shaped LSECC beam shells. Engineering Structures, 189, 618–634. doi:10.1016/j.engstruct.2019.03.097.

[21] Sabah, H. A. H., & Harba, I. S. I. (2021). A Review-Behavior of Reinforced Concrete Exterior Beam-Column Connections under Cyclic Loading. E3S Web of Conferences, 318. doi:10.1051/e3sconf/202131803008.

[22] Majumdar, M. R. B. A. (2022). Influence of Beam-Column Joint on the Seismic Response of RC Frames. International Journal for Research Trends and Innovation, 7(10), 97–106.

[23] Shen, X., Li, B., & Chen, Y. T. (2024). Seismic performance of reinforced concrete beam-column joints with diagonal bars wrapped by steel tubes: experimental, numerical and analytical study. Structures, 59. doi:10.1016/j.istruc.2023.105734.

[24] Şermet, F., Ercan, E., Hökelekli, E., & Arisoy, B. (2020). Cyclic Behavior of Composite Column-Reinforced Concrete Beam Joints. Sigma Journal of Engineering and Natural Sciences, 38(3), 1427–1445.

[25] Chen, L., Wang, Z., Ma, B., Peng, G., Wang, C., & Zhou, L. (2025). Seismic performance of a novel steel-concrete composite beam-column joint. Journal of Constructional Steel Research, 229(January), 109479. doi:10.1016/j.jcsr.2025.109479.

[26] Ghayeb, H. H., Ramli Sulong, N. H., Razak, H. A., & Mo, K. H. (2022). Enhancement of seismic behaviour of precast beam-to-column joints using engineered cementitious composite. Engineering Structures, 255, 113932. doi:10.1016/j.engstruct.2022.113932.

[27] Choi, H. K., Choi, Y. C., & Choi, C. S. (2013). Development and testing of precast concrete beam-to-column connections. Engineering Structures, 56, 1820–1835. doi:10.1016/j.engstruct.2013.07.021.

[28] Walpole, W. R. (1985). Beam-Column Joints. Bulletin of the New Zealand National Society for Earthquake Engineering, 18(4), 369–380. doi:10.5459/bnzsee.18.4.369-380.

[29] Akguzel, U., & Pampanin, S. (2010). Effect of axial load variation on the retrofit of exterior reinforced concrete beam-column joints. NZSEE Conference, 26-28 March, 2010, Wellington, New Zealand.

[30] Masi, A., Santarsiero, G., Mossucca, A., & Nigro, D. (2014). Influence of axial load on the seismic behavior of RC beam-column joints with wide beam. Applied Mechanics and Materials, 508, 208–214. doi:10.4028/www.scientific.net/AMM.508.208.

[31] Gan, D., Li, H., Zhou, Z., & Zhou, X. (2023). Effect of column flexural capacities and axial loads on bond behavior of interior beam-column joints. Engineering Structures, 289(October 2022), 116331. doi:10.1016/j.engstruct.2023.116331.

[32] Li, B., Lam, E. S. S., Wu, B., & Wang, Y. Y. (2015). Effect of high axial load on seismic behavior of reinforced concrete beam-column joints with and without strengthening. ACI Structural Journal, 112(6), 713–724. doi:10.14359/51687938.

[33] Al-Osta, M. A., Khan, U., Baluch, M. H., & Rahman, M. K. (2018). Effects of Variation of Axial Load on Seismic Performance of Shear Deficient RC Exterior BCJs. International Journal of Concrete Structures and Materials, 12(1), 1-20. doi:10.1186/s40069-018-0277-0.

[34] Haach, V. G., Lúcia Homce De Cresce El Debs, A., & Khalil El Debs, M. (2008). Evaluation of the influence of the column axial load on the behavior of monotonically loaded R/C exterior beam-column joints through numerical simulations. Engineering Structures, 30(4), 965–975. doi:10.1016/j.engstruct.2007.06.005.

[35] Bindhu, K. R., Sukumar, P. M., & Jaya, K. P. (2009). Performance of exterior beam-column joints under seismic type loading. ISET Journal of Earthquake Technology, 46(2), 47–64.

[36] Etemadi, E., & Vincent, T. (2017). Mechanical behavior of RC exterior wide beam-column joints under lateral loading: a parametric computational study. International Journal of Engineering and Technology, 9(3), 2003–2012. doi:10.21817/ijet/2017/v9i3/1709030153.

[37] Zhuang, M. L., Cheng, J., Fei, D., Sun, C., Wang, Z., Chen, B., & Qiao, Y. (2024). Numerical Simulation Study on the Seismic Performance of Prefabricated Fiber-Reinforced Concrete Beam–Column Joints with Grouted Sleeve Connections. International Journal of Concrete Structures and Materials, 18(1), 26. doi:10.1186/s40069-024-00671-2.

[38] Ašonja, A., Desnica, E., & Palinkaš, I. (2016). Analysis of the static behavior of the shaft based on finite element method under effect of different variants of load. Applied Engineering Letters, 1(1), 8–15.

[39] Xiao, Y., Yu, M., & Liu, W. (2024). Finite Element Analysis of Prefabricated Semi-Rigid Concrete Beam–Column Joint with Steel Connections. Applied Sciences (Switzerland), 14(12). doi:10.3390/app14125070.

[40] Birtel, V. A. M. P., & Mark, P. (2006). Parameterised finite element modelling of RC beam shear failure. ABAQUS users' conference, 23-25 Mat, 2006, Cambridge, United States.

[41] Nafees, A., Javed, M. F., Musarat, M. A., Ali, M., Aslam, F., & Vatin, N. I. (2021). FE Modelling and Analysis of Beam Column Joint Using Reactive Powder Concrete. Crystals, 11(11), 1372. doi:10.3390/cryst11111372.

[42] Sahil, M., Bahrami, A., Waqas, H. A., Amin, F., Mansoor Khan, M., Iqbal, F., Fawad, M., & Najam, F. A. (2024). Seismic performance evaluation of exterior reinforced concrete beam-column connections retrofitted with economical perforated steel haunches. Results in Engineering, 22(April), 102179. doi:10.1016/j.rineng.2024.102179.

[43] Jia, L.-J., & Kuwamura, H. (2014). Prediction of Cyclic Behaviors of Mild Steel at Large Plastic Strain Using Coupon Test Results. Journal of Structural Engineering, 140(2), 04013056. doi:10.1061/(asce)st.1943-541x.0000848.

[44] Amalia, A. R., Ochi, K., Tanaka, R., Kamachi, T., & Shiota, T. (2023). Comparison of hardening rules for numerical analysis of square hollow section under cyclic bending loading. Advances in Intelligent Applications and Innovative Approach, 2760, 020005. doi:10.1063/5.0129582.

[45] SNI-2847. (2019). Requirements for Structural Concrete for Building Structures. Standar Nasional Indonesia (SNI), Jakarta, Indonesia. (In Indonesian).

[46] ACI PRC-374.2-13. (2013). Guide for Testing Reinforced Concrete Structural Elements Under Slowly Applied Simulated Seismic Loads. American Concrete Institute (ACI), Farmington Hills, United States.